Heliyon 10 (2024) e38188

Contents lists available at ScienceDirect

Heliyon

journal homepage: www.cell.com/heliyon

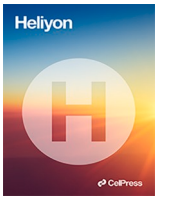

Research article

The mechanism of TGF-β mediating BRD4/STAT3 signaling pathway to promote fibroblast proliferation and thus promote keloid progression

Ruiqi Bai [1], Lixia Hao [1], Guiwen Zhou, Qiang Fu, Peixuan Zhang, Pianpian Lin, Minliang Chen [*]

Department of Plastic and Reconstructive Surgery, Senior Department of Burns and Plastic Surgery, The Forth Medical Center of Chinese PLA General Hospital, Beijing, 100142, China

ARTICLE INFO

Keywords:
Keloid
Fibroblasts
TGF-β
BRD4/STAT3 signaling pathway

ABSTRACT

Objective: The purpose of this study was to investigate the effect of TGF-β on keloid and its molecular mechanism in fibroblasts. Methods: The difference between normal tissue and keloid tissue can be detected using HE staining. Fibroblasts were treated with TGF-β, and then treated with the BRD4 inhibitor JQ1 and the STAT3 activator Colivelin TFA. Western blot was used to measure the relative protein expression of TGF-β, BRD4, p-STAT3, p-EZH2, C-myc, KLF2, KLF4, α-SMA, and Collagen-I. Immunofluorescence staining was used to measure the relative fluorescence intensity of BRD4, p-STAT3, α-SMA, and Collagen-I. Cell proliferation ability was evaluated by CCK-8 assay and colony formation assay. Results:The expression of TGF-β and BRD4 was significantly higher in keloid tissue compared to normal tissue. TGF-β mediated the BRD4/STAT3 signaling pathway to inhibit p-EZH2 and promote the expression of C-myc, KLF2, KLF4, α-SMA, and Collagen-I. Additionally, TGF-β mediated the BRD4/STAT3 signaling pathway to enhance fibroblast proliferation. Conclusion:TGF-β mediates the BRD4/STAT3 signaling pathway to promote fibroblast proliferation and contribute to the progression of keloid.

1. Introduction

keloid is a unique keloid-related disease in humans, characterized by excessive proliferation of fibroblasts and abnormal deposition of extracellular matrix. keloid often occurs after surgery, trauma, burns, or mosquito bites, and is clinically manifested as one or more non-self-limiting protrusions on the skin surface beyond the edge of the wound, which are most commonly found on the chest, back, shoulders, and ears. In the early stages of the disease, keloids are typically pink and gradually become pale over time, often accompanied by pigmentation. Due to the non-self-limiting growth of keloids and the accompanying itching and pain, they often cause significant psychological burden to patients [1,2]. Currently, the main treatment methods for keloid include surgical treatment, laser therapy, radiotherapy, cryotherapy, pressure therapy, and injection therapy. Although these treatment methods can delay the progression of keloids, the recurrence rate after treatment remains high [3–5]. Therefore, keloid has always been a focus and challenge in

* Corresponding author. Department of Plastic and Reconstructive Surgery, Senior Department of Burns and Plastic Surgery, the Forth Medical Center of Chinese PLA General Hospital, No.51, Fucheng Road, Baliizhuang Street, Haidian District, Beijing, 100142, China.
E-mail address: chenml@sohu.com (M. Chen).
[1] Ruiqi Bai and Lixia Hao are co-first authors.

https://doi.org/10.1016/j.heliyon.2024.e38188
Received 4 August 2024; Received in revised form 19 September 2024; Accepted 19 September 2024
Available online 21 September 2024

the diagnosis and treatment of plastic surgery diseases.

The formation of keloid is the result of abnormal wound healing. Wound healing mainly goes through three phases: inflammation phase, proliferation phase, and remodeling phase. The reconstruction of the skin begins at the time of injury. In the inflammatory phase, deactivated tissues are removed, fibroblasts migrate quickly, and blood vessels dilate in a cascade fashion. Activated platelets, endothelial cells, and macrophages release a range of cytokines that influence the migration, apoptosis, proliferation, and collagen production of normal or keloid fibroblasts. In the early stages of wound healing, fibroblasts are activated by local inflammatory factors, cytokines (e.g. TGF-β1, transforming growth factor β1). These cytokines initiate the process of differentiation of fibroblasts to myofibroblasts. Myofibroblasts are fibroblasts with smooth muscle cell-like characteristics that are primarily responsible for the production of extracellular matrix (ECM) and collagen and have the ability to contract wounds. They play an important role in the normal wound healing process, but in pathological conditions, myofibroblasts continue to activate and proliferate, leading to excessive collagen deposition and eventual keloid formation [6–8].

The family of cell factors known as Transforming proliferation Factor-β (TGF-β) is deeply engaged in the processes of tissue maturation, apoptosis, differentiation, and cell proliferation. There are two subgroups within the TGF-β family: the TGF-β/activin subgroup and the bone morphogenetic protein/growth and differentiation factor subgroup. The TGF-β/activin subgroup, which comprises two activins, inhibin and activin A, and three isoforms of TGF-β (TGF-β1, TGF-β2, and TGF-β3), is the subgroup most associated with fibrosis. TGF-β creates a reparative milieu for tissue repair during the wound healing process by enhancing the production of pro-fibrotic genes including type I collagen and connective tissue growth factor and inhibiting the breakdown of extracellular matrix [9,10]. BET proteins are key players in controlling gene transcription, DNA replication, damage, and repair. As "readers" of epigenetics, they primarily identify acetylated lysine residues in histone binding proteins. Two tandem bromodomains (BD1 and BD2) and an extra-terminal domain (ET) define them. This protein family includes BRD2, BRD3, BRD4, and BRDT in humans. Among them, BRD4 is widely expressed in mammalian tissues and cells. As a scaffold protein, BRD4 recruits many factors involved in gene expression regulation [11–13]. BRD4 has been discovered to have the ability to control the STAT3/EZH2 signalling pathway [14]. Therefore, the effect of TGF-β on keloid and its molecular mechanism through fibroblasts, mediated by the BRD4/STAT3 signaling pathway, has important therapeutic significance for keloid.

2. Methods

2.1. Bioinformatics analysis

Using R version 4.2.1, with the following R packages: GEOquery 2.64.2, limma 3.52.2, ggplot2 3.3.6, ComplexHeatmap 2.13.1. The dataset GSE145725 was downloaded from the GEO database using the GEOquery package. This dataset was an expression profiling chip, and the platform number was GPL16043 GeneChip® PrimeView™ Human Gene Expression Array (with External spike-in RNAs). The missing values in the data were supplemented using the impute package. Next, the normalizeBetweenArrays function from the limma package was used to conduct one more normalization of the data. When more than one probe corresponded to the same molecule, the probe with the highest signal value was retained and the other probes were eliminated. The ggplot2 package's box plots were used to display the data. The data underwent PCA analysis, and the ggplot2 software was used to visualise the results. The ggplot2 tool was used to visualise the findings of the differential analysis, with a threshold of $|\text{LogFC}|>1$ & $\text{p.adj}<0.05$. Row normalization was performed, the row clustering was set to Euclidean distance, and column clustering was not performed. Finally, the heatmap was visualized using the ComplexHeatmap package.

Using R version 4.2.1, with the following R packages: clusterProfiler 4.4.4, GOplot 1.0.2, ggplot2 3.3.6, ID conversion package: org.Hs.eg.db. Species: Homo sapiens. After converting the input molecule list using the ID conversion package, enrichment analysis was performed using the clusterProfiler package. Z-score values for each enrichment term were calculated using the provided numerical values and the GOplot package. A threshold of $\text{p.adj}<0.05$ was set, and gene clusters and pathways with biological feature differences among differentially expressed genes were identified. The ggplot2 software was used to visualise the findings of the enrichment study. Moreover, Gene Set Enrichment Analysis (GSEA) on the MSigDB Collections gene set database was used to confirm the GOKEGG enrichment analysis findings using the clusterProfiler program.

Using R version 4.2.1, with the following R packages: ggplot2 3.3.6, stats 4.2.1, car 3.1-0. Based on the data format characteristics, the Spearman statistical method was chosen for analysis. The ggplot2 software was used to visualise the data. The genes STAT3 (Signal Transducer And Activator Of Transcription 3), P38 (p38 mitogen-activated protein kinase), BRD4 (Bromodomain Containing 4), and EZH (Enhancer Of Zeste 2 Polycomb Repressive Complex 2 Subunit) were specifically examined using scatter plots.

2.2. Experimental materials

A total of 30 patients diagnosed with keloid in the Forth Medical Center of Chinese PLA General Hospital between 2023 and 2024 were selected, aged 20–50 years, including 20 males and 10 females. Normal tissue and keloid tissue were collected according to the guidelines of Medical Ethics Committee for Clinical Trials at the Forth Medical Center of Chinese PLA General Hospital, and all specimens were obtained with patient informed consent and signed informed consent forms. The specimens were separated into two sections, one of which was utilised for the tests that followed and the other of which was immediately kept in a freezer set at −80 °C.

2.3. HE staining

A dye solution was used to colour the 4 μm-thick sections of paraffin-embedded scar tissue. The sections were washed and stained with hematoxylin-eosin staining solution (Thermo Fisher) for 3 min, followed by differentiation with hydrochloric acid-alcohol

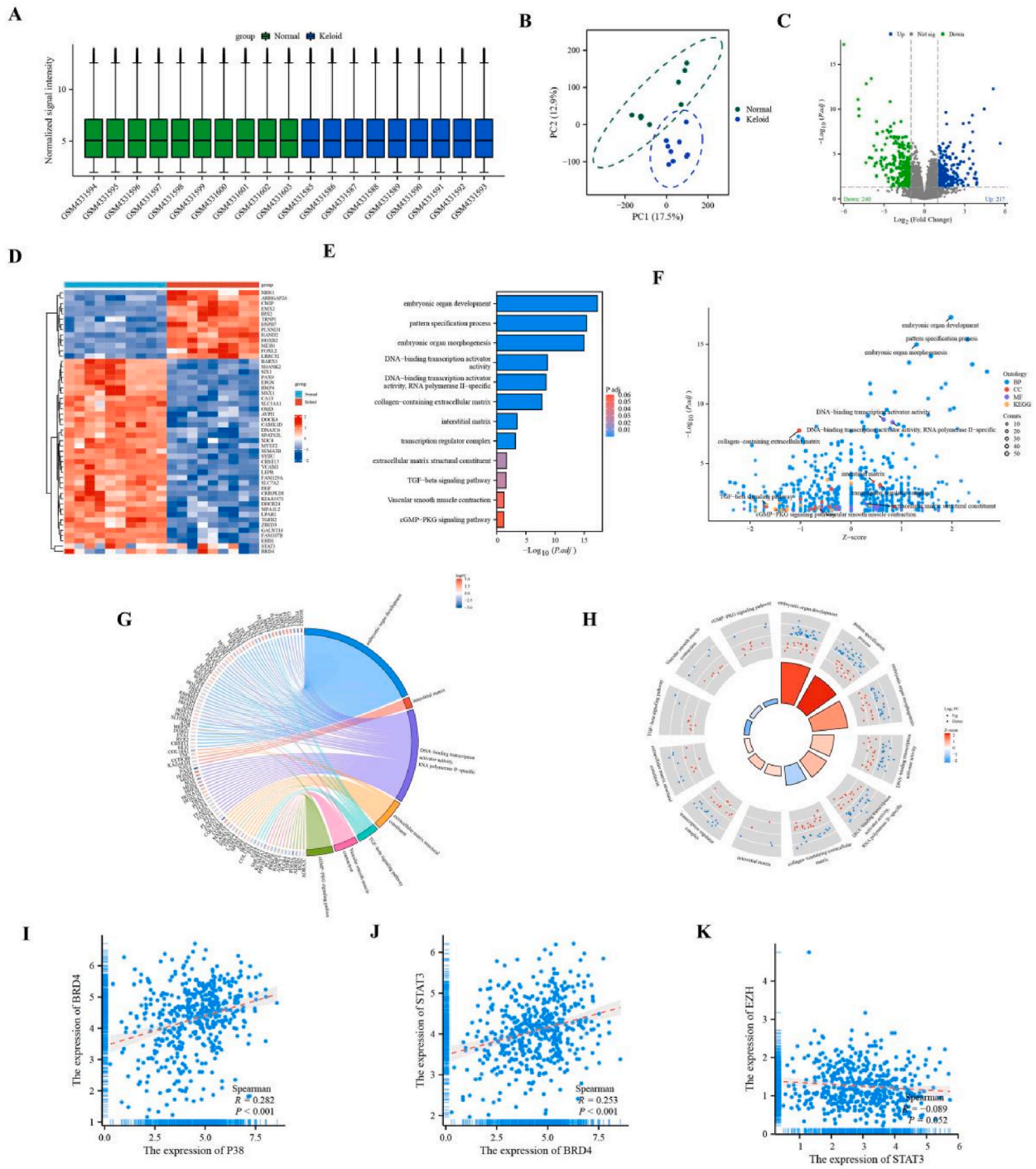

Fig. 1. Results of bioinformatics analysis.
A: Box plot analysis of the samples; B: PCA plot analysis; C: Volcano plot showing the results of differential analysis; D: Heatmap visualization; E-H: Bar plot, bubble plot, chord diagram, and circular plot visualizing the results of GOKEGG enrichment analysis; I: Scatter plot of P38 and BRD4; J: Scatter plot of BRD4 and STAT3; K: Scatter plot of STAT3 and EZH.

differentiation solution. The sections were then counterstained with saturated sodium phosphate solution for 10 min, placed in ethanol, and subsequently treated with eosin solution for 30 s. After drying, they were mounted with neutral mounting medium.

2.4. Fibroblast culture

Primary fibroblasts were isolated and cultured from human keloid tissue. Tissue samples were harvested, cut into small pieces, and digested with 0.3 % type I collagenase. The digested tissue samples were filtered through a 200 μm mesh and centrifuged at 500×*g* for 10 min. After dikeloidding the supernatant, the pellet was again suspended in DMEM with 10 % foetal bovine serum, and it was cultivated in 5 % CO2 at 37 °C. Primary fibroblasts of passage 2–3 were used for the experiments. Fibroblasts were treated with TGF-β and divided into control group and TGF-β group. The control group and TGF-β group were treated with the BRD4 inhibitor JQ-1 and the STAT3 activator Colivelin TFA, respectively.

2.5. CCK-8 assay

The Cell Counting Kit-8 assay (CCK-8 assay, Sigma) was used to quantify the cell proliferation of fibroblasts in compliance with the manufacturer's guidelines. In a 96-well plate, fibroblasts were planted at a density of 3000 cells/well. Absorbance was measured at 450 nm at designated time points.

2.6. Immunofluorescence staining

After being fixed for 30 min in 4 % paraformaldehyde, the cells were treated for 10 min to improve antibody penetration with 0.1 % Triton X-100 in PBS and three PBS washes. Blocking was performed with 5 % bovine serum albumin for 1 h, followed by incubation with primary antibodies against BRD4, p-STAT3, α-SMA, and collagen-I overnight at 4 °C. After washing, cells were incubated with fluorescent goat anti-rabbit secondary antibodies in the dark for 2 h. Slides were mounted in the dark, and observations were made under a fluorescence microscope.

2.7. Western Blotting

Fibroblasts were digested with trypsin, washed with PBS, and lysed with RIPA lysis buffer to prepare total cellular proteins. Protein concentration was measured using the BCA method. Samples were mixed with loading buffer, boiled in a metal bath for 10 min. Proteins (20 μg/well) were separated by SDS-PAGE and transferred onto PVDF membranes. The membranes were blocked with 5 % skim milk at room temperature for 2 h, followed by incubation with primary antibodies against TGF-β, BRD4, p-STAT3, p-EZH2, C-myc, KLF2, KLF4, α-SMA, and Collagen-I overnight at 4 °C. On the second day, after washing the membranes with TBST, HRP-conjugated secondary antibodies were incubated at room temperature for 2 h. After washing with TBST, an appropriate amount of ECL luminescent solution was added. Exposures were performed and grayscale values were analyzed using a gel imaging system.

2.8. Statistical analysis

GraphPad Prism 9.0 software was used for data analysis and plotting. Quantitative data were presented as mean ± standard deviation (SD). Independent sample data comparison was performed using unpaired *t*-test, and one-way analysis of variance (ANOVA) was used for multiple group comparisons. $P < 0.05$ was considered statistically significant.

3. Results

3.1. Results of bioinformatics analysis

In the dataset GSE145725, 19 groups of samples were divided into two groups: 9 samples in the scar tissue group and 10 samples in the normal group. Through box plots (Fig. 1A), it was observed that the samples were well normalized. PCA plot (Fig. 1B) revealed significant differences between the two groups of samples. The differential analysis findings were shown in a volcano map (Fig. 1C), where 217 blue dots indicated highly upregulated genes, 240 green dots indicated considerably downregulated genes, and 18586 grey dots indicated genes with no significant changes. A heatmap (Fig. 1D) was generated to visualise the expression of the 457 differentially expressed molecules, where blue represented significantly upregulated genes and green represented significantly downregulated genes.

The input molecule list was converted to Entrez IDs for GOKEGG enrichment analysis. A total of 457 IDs were entered, out of which 425 were successfully converted to Entrez IDs, with a conversion rate of 93 %. GOKEGG analysis of the corresponding differentially expressed genes was performed to integrate GO terms and create a biological process network for the differentially expressed genes. The functional annotation results from GOKEGG were categorized into three classes: Biological Process (BP), Cellular Component (CC), and Molecular Function (MF). The results of GOKEGG enrichment analysis were visualized using bar plots (Fig. 1E), bubble plots (Fig. 1F), chord diagrams (Fig. 1G), and circular plots (Fig. 1H). Among the differentially expressed genes, the top 12 enriched pathways in terms of BP, CC, and MF were linked to biological processes such the TGF-beta signalling system, vascular smooth muscle contraction, and renin secretion.

Scatter plots of P38 and BRD4 (Fig. 1I) demonstrated that P38 promotes the expression of BRD4. Scatter plots of BRD4 and STAT3 (Fig. 1J) revealed that BRD4 enhances the expression of STAT3. Scatter plots of STAT3 and EZH (Fig. 1K) indicated that STAT3 inhibits the expression of EZH.

3.2. Impact of TGF-β on BRD4/STAT3 signalling pathway-related protein production in keloid fibroblasts

First, the results of HE staining showed that the area of keloid tissue in the keloid tissue was significantly larger compared to normal tissue (Fig. 2A and B).Keloid tissue typically exhibits a disorganized and dense arrangement of collagen fibers, while normal tissue has a more organized and regular structure. Keloid tissue may have increased cell density, with the presence of fibroblasts and inflammatory cells, whereas normal tissue usually has lower cell density. Keloid tissue may show signs of chronic inflammation, such as the presence of immune cells and cytokines, while normal tissue generally does not exhibit significant inflammation. Due to the disrupted structure and composition, keloid tissue may have impaired function compared to normal tissue.

To determine if the necessary proteins were expressed in fibroblasts, Western blot analysis was done. The findings demonstrated that the TGF-β group's relative protein expression levels of TGF-β, BRD4, p-STAT3, C-myc, KLF2, and KLF4 were much higher than those of the control group, whereas the relative protein expression of p-EZH2 was dramatically lowered. Following treatment of the fibroblasts in both the TGF-β group and control group with the BRD4 inhibitor JQ-1, there was a considerable rise in the relative protein expression of p-EZH2, and the significant difference was no longer present. TGF-β, BRD4, p-STAT3, C-myc, KLF2, and KLF4 relative protein expression levels were dramatically reduced, and the significant difference was abolished. Following treatment of the fibroblasts with the STAT3 activator Colivelin TFA in the TGF-β+JQ-1 group as well as the control + JQ-1 group, there was no discernible change in the relative BRD4 protein expression. After a considerable drop in the relative protein expression of p-EZH2, the significant difference was no longer present. TGF-β, p-STAT3, C-myc, KLF2, and KLF4 relative protein expression levels were dramatically elevated, and the significant difference was abolished (Fig. 3A).

Using immunofluorescence staining, the relative fluorescence intensity of p-STAT3 and BRD4 in fibroblasts was measured. The relative fluorescence intensity of BRD4 and p-STAT3 was found to be considerably higher in the TGF-β group as compared to the control group. Following administration of the BRD4 inhibitor JQ-1 to the fibroblasts in both the TGF-β group and the control group, there was a considerable reduction in the relative fluorescence intensity of BRD4 and p-STAT3, and the statistical difference was abolished. Following treatment of the fibroblasts with the STAT3 activator Colivelin TFA in the TGF-β+JQ-1 group as well as the control + JQ-1 group, there was no discernible change in the relative BRD4 protein expression. The considerable difference was removed and p-STAT3's relative fluorescence intensity rose dramatically (Fig. 3B).

3.3. Effects of TGF-β mediated BRD4/STAT3 signaling pathway on fibroblast proliferation

CCK-8 assay results showed that at 72 h, the OD value in the TGF-β group was significantly higher compared to the control group.

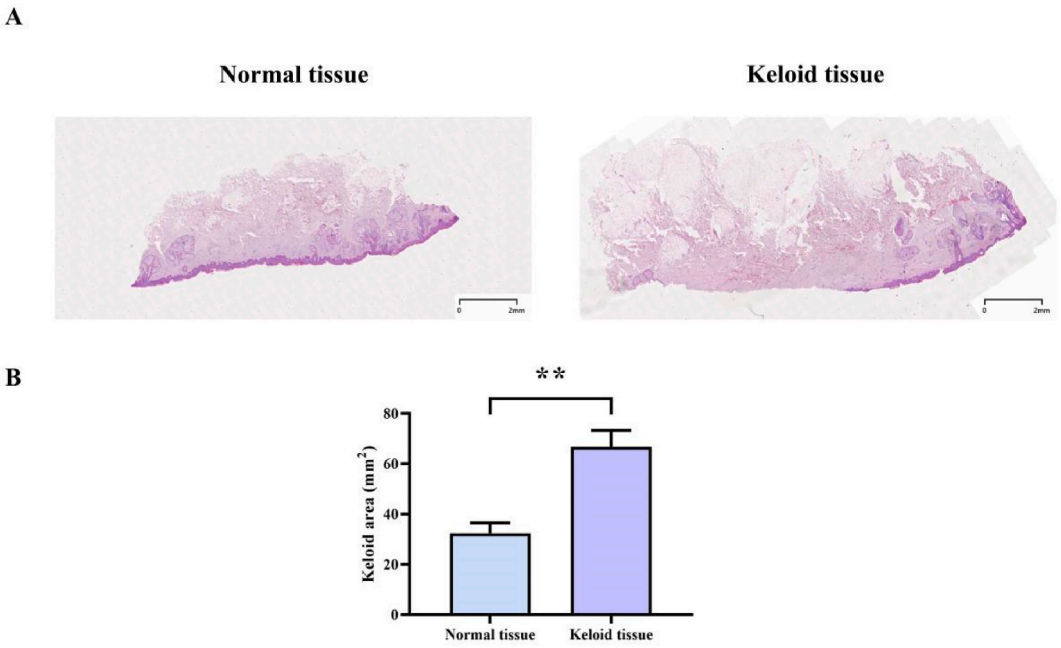

Fig. 2. The differences between scar tissue and normal tissue.
A:HE staining results in normal tissue and keloid tissue; B:Keloid area statistics. Data are expressed as mean ± standard deviation; Normal tissue vs Keloid tissue: **P < 0.01.

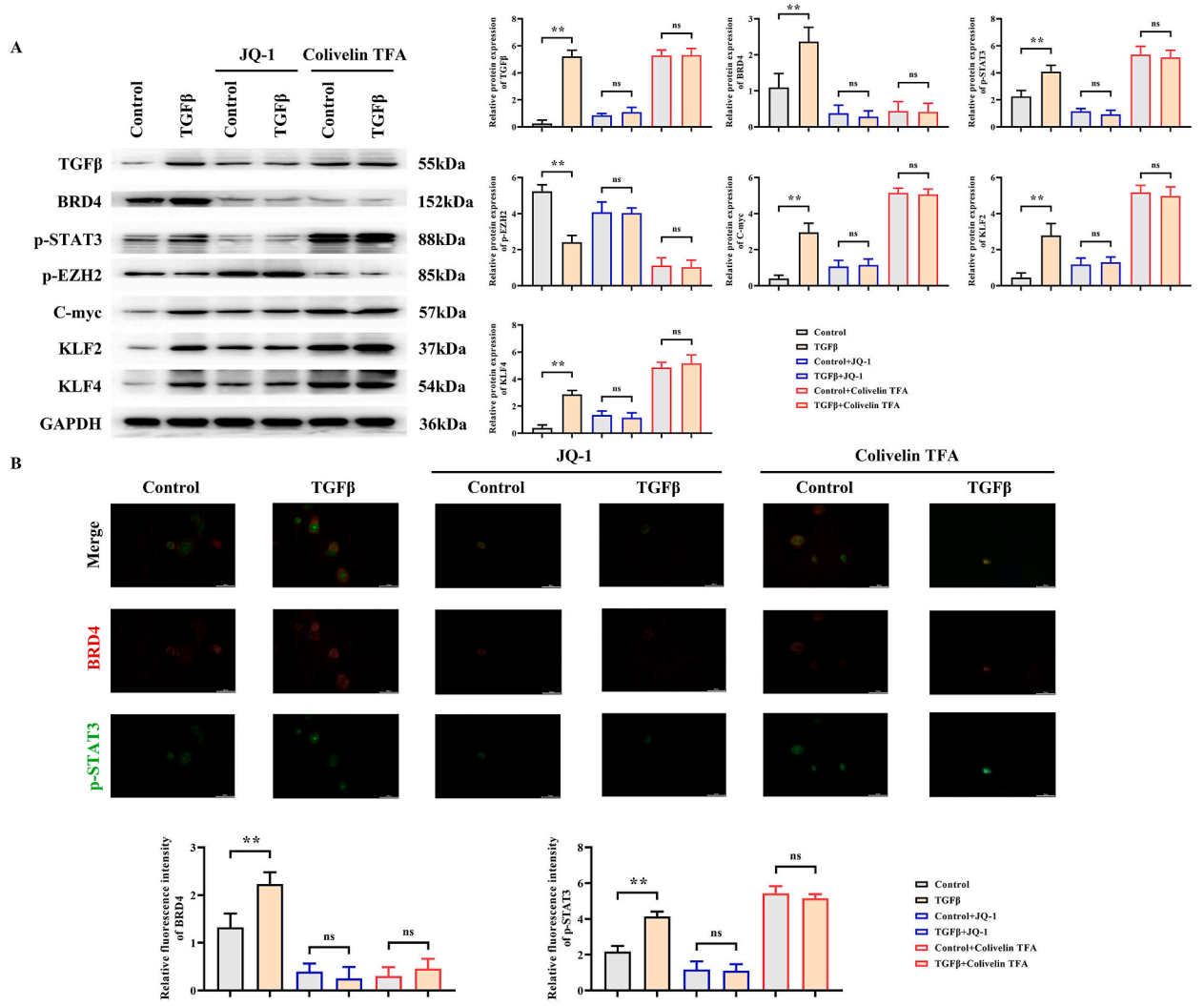

Fig. 3. Effect of TGFβ on the expression of BRD4/STAT3 signaling pathway-related proteins in keloid fibroblasts.
A: Protein band graphs and relative protein expression levels of TGFβ, BRD4, p-STAT3, p-EZH2, C-myc, KLF2, and KLF4; GAPDH as control protein; B: Immunofluorescence staining results and relative fluorescence intensity of BRD4 and p-STAT3. Red: BRD4; Green: p-STAT3; Data are expressed as mean ± standard deviation; Control group vs TGFβ group: **P < 0.01; Control + JQ-1 group vs TGFβ+JQ-1 group: ^{ns}P>0.05; Control + Colivelin TFA group vs TGFβ+Colivelin TFA group: ^{ns}P>0.05.

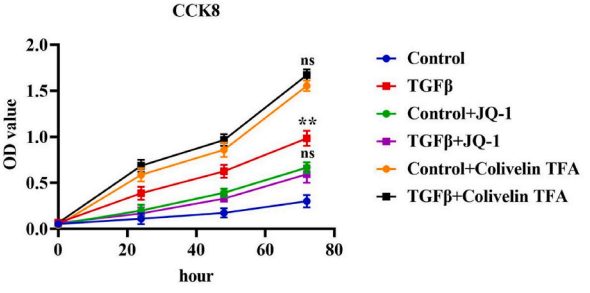

Fig. 4. CCK-8 assay detects the effect of TGFβ-mediated BRD4/STAT3 signalling pathway on fibroblast proliferation.
Data are expressed as mean ± standard deviation; Control group vs TGFβ group: **P < 0.01; Control + JQ-1 group vs TGFβ+JQ-1 group: ^{ns}P>0.05; Control + Colivelin TFA group vs TGFβ+Colivelin TFA group: ^{ns}P>0.05.

After treating the fibroblasts with the BRD4 inhibitor JQ-1 in both the control group and TGF-β group, the OD values were significantly decreased, and the significant difference was eliminated. After treating the fibroblasts with the STAT3 activator Colivelin TFA in both the control + JQ-1 group and TGF-β+JQ-1 group, the OD values were significantly increased, and the significant difference was eliminated (Fig. 4).

3.4. *Effects of TGF-β mediated BRD4/STAT3 signaling pathway on the expression of α-SMA and Collagen-I*

Western blot examination revealed a substantial increase in the relative protein expression levels of Collagen-I and α-SMA in the TGF-β group as compared to the control group. Following administration of the BRD4 inhibitor JQ-1 to the fibroblasts in both the TGF-β group and the control group, there was a considerable reduction in the relative protein expression levels of α-SMA and Collagen-I, and the statistical difference was abolished. Following administration of the STAT3 activator Colivelin TFA to the fibroblasts in the TGF-β+JQ-1 group as well as the control + JQ-1 group, there was a substantial reduction in the significant difference between the relative protein expression levels of α-SMA and Collagen-I (Fig. 5A).

According to the findings of immunofluorescence staining, the TGF-β group had a considerable rise in the relative fluorescence intensity of α-SMA and Collagen-I when compared to the control group. Following administration of the BRD4 inhibitor JQ-1 to the fibroblasts in the TGF-β group as well as the control group, there was a considerable reduction in the relative fluorescence intensity of α-SMA and Collagen-I, and the statistical difference was abolished. Following administration of the STAT3 activator Colivelin TFA to the fibroblasts in the TGF-β+JQ-1 group as well as the control + JQ-1 group, there was no longer a significant difference in the relative fluorescence intensity of α-SMA and Collagen-I (Fig. 5B). These results demonstrate that TGF-β mediated the BRD4/STAT3 signaling pathway to promote fibroblast proliferation and contribute to the progression of keloid (Fig. 6). The complete gels and blots from this study were supplemented in Supplementary Fig. 1.

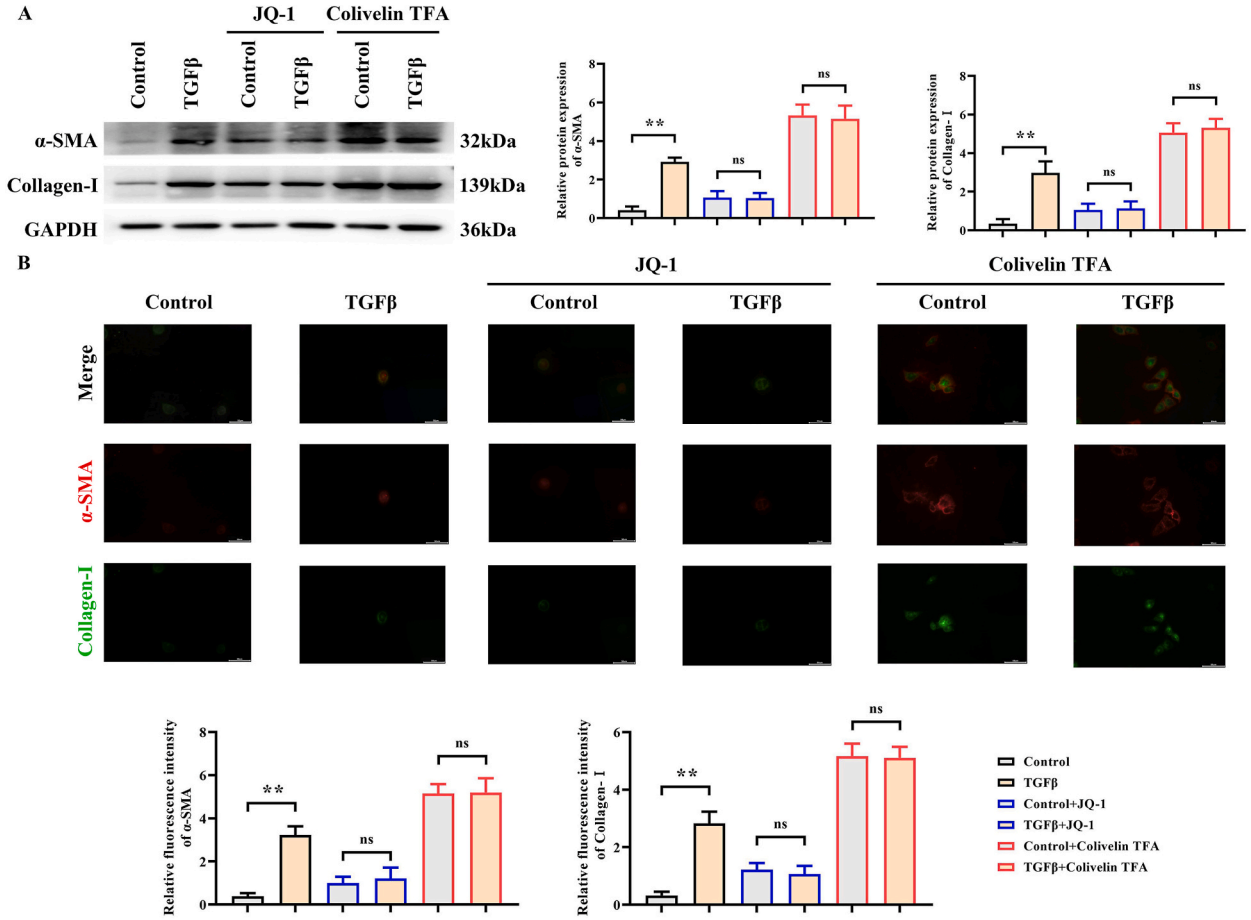

Fig. 5. Effect of TGFβ-mediated BRD4/STAT3 signaling pathway on the expression of α-SMA and Collagen-I.
A: Protein band graphs and relative protein expression levels of α-SMA and Collagen-I; GAPDH as control protein; B: Immunofluorescence staining results and relative fluorescence intensity of α-SMA and Collagen-I. Red: α-SMA; Green: Collagen-I; Data are expressed as mean ± standard deviation; Control group vs TGFβ group: **P < 0.01; Control + JQ-1 group vs TGFβ+JQ-1 group: ^{ns}P>0.05; Control + Colivelin TFA group vs TGFβ+Colivelin TFA group: ^{ns}P>0.05.

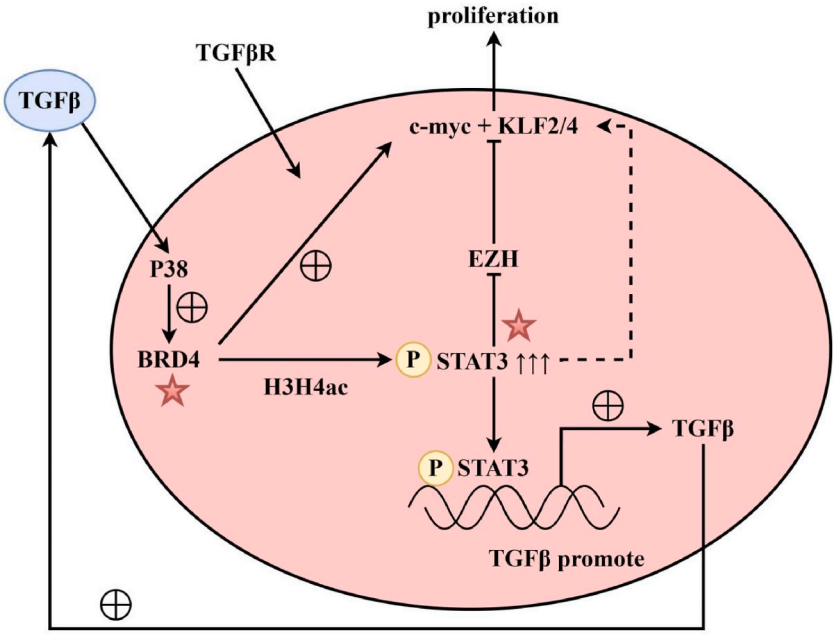

Fig. 6. Promotion of fibroblast proliferation and progression of keloid tissue by TGFβ-mediated BRD4/STAT3 signaling pathway.

4. Discussion

Under the stimulation of chronic inflammation, fibroblasts in keloid tissue increase the expression of pro-fibrotic cytokines and decrease the expression of inhibitory cell fibrotic factors. This process ultimately leads to pathological fibrosis of keloids. According to their secretion sources, pro-fibrotic factors include transforming growth factor β1 (TGF-β1), transforming growth factor β2 (TGF-β2), vascular endothelial growth factor (VEGF), etc. After 2–3 days of inflammatory phase, wound healing enters the proliferation phase, where cell proliferation and migration become active, which are typical characteristics of this stage. These proliferating fibroblasts synthesize extracellular matrix (ECM), mainly in the form of type I collagen (COL-I) and type III collagen (COL-III). At the same time, some fibroblasts are influenced by TGF-B1 and differentiate into myofibroblasts, leading to upregulation of a-SMA expression. Due to the contractile nature of fibroblasts, they secrete large amounts of collagen protein while differentiating into myofibroblasts, resulting in the formation of initial keloids during wound healing [15–17]. Research has found that activation of the P38 signaling pathway can promote the transcription of fibrotic genes such as type I collagen protein and smooth muscle actin (a-SMA), leading to tissue fibrosis [18–20]. More studies have confirmed that inhibition of the TGF-B1/p38 pathway can alleviate tissue or organ fibrosis.

Proteins containing bromodomain structures can be divided into 9 families, with the BET family being the largest and most extensively studied. The BRD2, BRD3, BRD4, and tissue-specific BRDt proteins are members of the BET family. These proteins contain two common bromodomain structures (BD1 and BD2) at their N-terminus. As readers of protein acetylation, BET proteins bind to acetylated lysine residues via BD1 and BD2, recognising acetylated histones and regulating transcriptional activity. In order to control the transcription of genes, the N- and C-terminal domains of BET proteins may interact with chromatin modification enzymes and transcription factors, bringing these co-regulatory factors to enhancer or promoter locations. These proteins, which are found in the cell nucleus, control a variety of biological processes, including as DNA replication and gene transcription [21,22]. However, the functional differences between them are not yet clear. In this study, we found significantly higher expression of TGFβ and BRD4 in keloid tissue compared to normal tissue. Therefore, BRD4 is an important target for the treatment of keloid tissue.

Signal transducers and activators of transcription 3 (STAT3) is a transcription factor that is involved in key cellular processes related to cell cycle progression and anti-apoptosis programs. Upon stimulation by cytokines, STAT3 is activated and enters the cell nucleus, leading to the transcription of different downstream target genes [23]. It has been found that BRD4 can promote the activation of STAT3. Enhancer of zeste homolog 2 (EZH2) is a core subunit of the polycomb repressive complex 2 (PRC2) with catalytic activity, and it can catalyze the trimethylation of histone H3 lysine 27 (H3K27me3), which leads to the silencing of corresponding genes. EZH2 is involved in tumor proliferation, invasion, metastasis, drug resistance, etc., and is negatively correlated with the prognosis of cancer patients. Recently, some studies have found that STAT3 can inhibit the activation process of EZH2. EZH2 can inhibit the expression of c-myc [24,25].

C-Myc is an oncogene in the myc transcription factor family. It has 2 introns and 3 exons, with only exons 2 and 3 encoding functional proteins. The transcription factor encoded by the c-Myc gene regulates the expression of 15 % of genes by binding to enhancer box sequences (E-box) and histone acetyltransferases (HATs). The c-Myc transcription factor is an upstream regulatory factor in the cell cycle and plays a role in the transition process from the G1/S phase by regulating the transcription level of target genes [26,27]. In addition, c-Myc can also regulate DNA synthesis by interacting with the pre-replicative complex (pre-RC). Klf4 is an oncogene

that encodes a protein homologous to the Drosophila melanogaster Krüppel protein. It belongs to the Krüppel-like family of transcription factors and plays an important role in cell proliferation, differentiation, and survival. Klf4 has three domains: a DNA-binding domain, a transcription regulatory domain, and a nuclear localization sequence. The transcription regulatory domain at the amino terminus is rich in proline and serine and mainly has inhibitory or activating effects on transcription. The DNA-binding domain at the carboxy terminus is highly conserved and contains three zinc finger structures, which are mainly involved in specific binding to DNA. Klf4 can interact with basic transcription elements SP1 elements or CACCC elements located in the promoter region, thereby regulating the transcription level of downstream target genes and causing a series of biological reactions [28–30]. Therefore, in this study, we found that TGFβ can mediate the expression of BRD4/STAT3 signaling pathway, inhibit p-EZH2, promote the expression of C-myc, KLF2, KLF4, α-SMA, and Collagen-I. And TGFβ can mediate the BRD4/STAT3 signaling pathway to promote the proliferative ability of fibroblasts.

In conclusion, TGFβ mediates the BRD4/STAT3 signaling pathway to promote the proliferation of fibroblasts and the progression of keloid tissue, providing a new therapeutic target for the treatment of keloid tissue. However, targeting the BRD4/STAT3 signalling pathway may also pose some potential challenges and limitations.BRD4 and STAT3 do not only play a role in keloid formation, but they are also involved in a variety of other biological processes, including normal cell proliferation, immune response and tissue repair. Therefore, inhibitors targeting BRD4/STAT3 may affect normal cellular functions and lead to side effects. Cellular responses to BRD4/STAT3 inhibitors may vary and resistance may develop especially during long-term treatment. In topical treatments, drug delivery systems need to be designed to ensure effective penetration of the drug and long-lasting effects in the keloid tissue without affecting the surrounding healthy tissue. Keloid scarring is a chronic pathological process that may require long-term treatment, and it is still not entirely clear whether long-term inhibition of the BRD4/STAT3 pathway will result in drug resistance or other long-term side effects. Although specific therapies against BRD4/STAT3 are still in the research phase in keloid treatment, inhibitors against these two targets have already had applications in other areas, particularly in anti-cancer and anti-fibrotic therapies.BRD4 inhibitors have already been clinically investigated in certain cancers (e.g., leukaemia, lymphoma) and have shown some efficacy.BET inhibitors can be used to inhibit the BRD4 pathway by inhibiting the activity of the transcription factor BRD4, reducing the proliferation and survival of tumour cells. The same inhibitory strategy has the potential to be used to inhibit hyperproliferative fibroblasts in keloids. However, due to their systemic effects, the safety of these drugs in non-tumourous diseases needs to be further evaluated.Inhibitors of STAT3 (e.g., small molecule inhibitors, siRNAs, etc.) have found initial application in anti-tumour and anti-inflammatory therapies.STAT3 is activated in a wide range of cancers and chronic inflammatory diseases, making it a potential therapeutic target. In keloids, targeting STAT3 has the potential to inhibit fibrosis and abnormal deposition of extracellular matrix. Targeting the BRD4/STAT3 signalling pathway has great potential in keloid therapy, especially in inhibiting abnormal fibroblast proliferation and collagen overproduction. Therapies targeting the TGF-β pathway have made some progress in antifibrotic research. However, TGF-β has a wide range of roles in a variety of tissue repair and immunomodulatory processes, and targeting this pathway may cause side effects. In contrast, the BRD4/STAT3 signalling pathway is more downstream and targeting it may be more specific, but faces similar issues of systemic effects. Moreover, some existing antifibrotic drugs (e.g. pirfenidone, nidanib) have been approved for the treatment of diseases such as idiopathic pulmonary fibrosis, and these drugs work by inhibiting multiple fibrotic pathways. However, they typically act broadly and may affect multiple cellular processes simultaneously. In contrast, strategies targeting BRD4/STAT3 are more specific and may be superior in inhibiting hyperfibrosis, but may also be more susceptible to developing resistance or evading drug action through compensatory pathways. We will therefore validate the efficacy of BRD4/STAT3 inhibitors in vivo using a mouse keloid model. By inhibiting these signalling pathways, the effects on scar volume, collagen deposition and inflammatory response were observed. This will allow verification of whether these pathways have therapeutic potential under actual pathological conditions.

Ethics statement

The study was approved by the Medical Ethics Committee for Clinical Trials of the Forth Medical Center of Chinese PLA General Hospital.(2024KY060-KS001)

Data availability

The data that support the findings of this study are available on request from the corresponding author.

Funding

None.

CRediT authorship contribution statement

Ruiqi Bai: Writing – original draft, Validation, Software, Resources, Funding acquisition, Formal analysis, Conceptualization. **Lixia Hao:** Writing – original draft, Software, Project administration, Methodology, Investigation, Funding acquisition, Formal analysis, Data curation, Conceptualization. **Guiwen Zhou:** Supervision, Software, Resources, Project administration, Methodology, Formal analysis, Data curation, Conceptualization. **Qiang Fu:** Visualization, Validation, Resources, Methodology, Investigation, Funding acquisition, Data curation, Conceptualization. **Peixuan Zhang:** Resources, Project administration, Methodology, Investigation, Funding acquisition. **Pianpian Lin:** Software, Resources, Project administration, Methodology, Investigation, Data curation,

Conceptualization. **Minliang Chen:** Writing – review & editing, Validation, Resources, Project administration, Methodology, Funding acquisition, Formal analysis, Data curation, Conceptualization.

Declaration of competing interest

The authors declare that they have no known competing financial interests or personal relationships that could have appeared to influence the work reported in this paper.

Acknowledgements

None.

Appendix A. Supplementary data

Supplementary data to this article can be found online at https://doi.org/10.1016/j.heliyon.2024.e38188.

References

[1] Y. Zhong, Y. Zhang, B. Lu, Z. Deng, Z. Zhang, Q. Wang, J. Zhang, Hydrogel loaded with components for therapeutic applications in hypertrophic scars and keloids, International journal of nanomedicine 19 (2024) 883–899.
[2] Y. Zhong, Y. Zhang, A. Yu, Z. Zhang, Z. Deng, K. Xiong, Q. Wang, J. Zhang, Therapeutic role of exosomes and conditioned medium in keloid and hypertrophic scar and possible mechanisms, Front. Physiol. 14 (2023) 1247734.
[3] S.Y. Zhao, D. Wu, C. Cheng, J.H. Xie, Advances and future directions in keloid research: pathogenesis, diagnosis and personalized treatment strategies, World journal of clinical cases 11 (34) (2023) 8094–8098.
[4] X. Zhang, X. Wu, D. Li, The communication from immune cells to the fibroblasts in keloids: implications for immunotherapy, Int. J. Mol. Sci. 24 (20) (2023).
[5] M.Z. Zhang, X.H. Dong, W.C. Zhang, D.L. Pan, L. Ding, H.R. Li, P.X. Zhao, M.Y. Liu, L.B. Si, X.J. Wang, X. Long, Y.F. Liu, A new photodynamic therapy photosensitizer (p1) promotes apoptosis of keloid fibroblasts by targeting caspase-8, Journal of plastic surgery and hand surgery 57 (1–6) (2023) 324–329.
[6] Y. Zhou, Y. Sun, W. Hou, L. Ma, Y. Tao, D. Li, C. Xu, J. Bao, W. Fan, The JAK2/STAT3 pathway inhibitor, AG490, suppresses the abnormal behavior of keloid fibroblasts in vitro, Int. J. Mol. Med. 46 (1) (2020) 191–200.
[7] W. Zheng, G. Lin, Z. Wang, Bioinformatics study on different gene expression profiles of fibroblasts and vascular endothelial cells in keloids, Medicine 100 (47) (2021) e27777.
[8] X. Zhao, X. Jie, Y.K. Gao, B. Nie, H. Jiang, Long non-coding RNA CACNA1G-AS1 promotes proliferation and invasion and inhibits apoptosis by regulating expression of miR-205 in human keloid fibroblasts, Biosci. Rep. 40 (6) (2020).
[9] R. Yuan, X. Dai, Y. Li, C. Li, L. Liu, Exosomes from miR-29a-modified adipose-derived mesenchymal stem cells reduce excessive scar formation by inhibiting TGF-β2/Smad3 signaling, Mol. Med. Rep. 24 (5) (2021).
[10] Z.Y. Wu, H.J. Zhang, Z.H. Zhou, Z.P. Li, S.M. Liao, Z.Y. Wu, H.H. Huang, Y.C. Shi, The effect of inhibiting exosomes derived from adipose-derived stem cells via the TGF-β1/Smad pathway on the fibrosis of keloid fibroblasts, Gland Surg. 10 (3) (2021) 1046–1056.
[11] W. Zhu, R.D. Wu, Y.G. Lv, Y.M. Liu, H. Huang, J.Q. Xu, BRD4 blockage alleviates pathological cardiac hypertrophy through the suppression of fibrosis and inflammation via reducing ROS generation, Biomedicine & pharmacotherapy = Biomedecine & pharmacotherapie 121 (2020) 109368.
[12] J.X. Zhou, E. Agborbesong, L.X. Li, X. Li, Bromodomain protein BRD4-mediated mutant p53 transcription promotes TNBC progression, Int. J. Mol. Sci. 23 (23) (2022).
[13] D. Zhou, W. Liu, J. Zhang, Y. Dong, J. Wu, Y. Zhang, C. Dai, T. Zhang, G. Yang, Y. Zhang, A. Li, Bellidifolin ameliorates isoprenaline-induced cardiac hypertrophy by the Nox4/ROS signalling pathway through inhibiting BRD4, Cell death discovery 9 (1) (2023) 279.
[14] M.L. Fisher, S. Balinth, Y. Hwangbo, C. Wu, C. Ballon, J.E. Wilkinson, G.L. Goldberg, A.A. Mills, BRD4 regulates transcription factor ΔNp63α to drive a cancer stem cell phenotype in squamous cell carcinomas, Cancer Res. 81 (24) (2021) 6246–6258.
[15] Y. Zhang, X. Li, W. Liu, G. Hu, H. Gu, X. Cui, D. Zhang, W. Zeng, Y. Xia, TWEAK/Fn14 signaling may function as a reactive compensatory mechanism against extracellular matrix accumulation in keloid fibroblasts, European journal of cell biology 102 (2) (2023) 151290.
[16] X. Le, Y.F. Fan, ADAM17 regulates the proliferation and extracellular matrix of keloid fibroblasts by mediating the EGFR/ERK signaling pathway, Journal of plastic surgery and hand surgery 57 (1–6) (2023) 129–136.
[17] L. He, C. Zhu, H. Dou, X. Yu, J. Jia, M. Shu, Keloid core factor CTRP3 overexpression significantly controlled TGF-β1-induced propagation and migration in keloid fibroblasts, Dis. Markers 2023 (2023) 9638322.
[18] B.Y. Zhou, W.B. Wang, X.L. Wu, W.J. Zhang, G.D. Zhou, Z. Gao, W. Liu, Nintedanib inhibits keloid fibroblast functions by blocking the phosphorylation of multiple kinases and enhancing receptor internalization, Acta Pharmacol. Sin. 41 (9) (2020) 1234–1245.
[19] N. Zhu, B. Huang, L. Zhu, Bibliometric analysis of the inflammation in diabetic cardiomyopathy, Frontiers in cardiovascular medicine 9 (2022) 1006213.
[20] Q. Zhou, Q. Zhou, Q. Liu, Z. He, Y. Yan, J. Lin, Z. Chen, C. He, K. Mao, J. Wang, Z. Zhou, Z. Xiao, J. Zhang, PRL-3 facilitates Hepatocellular Carcinoma progression by co-amplifying with and activating FAK, Theranostics 10 (22) (2020) 10345–10359.
[21] Z. Tan, Z. Wang, Q. Zeng, X. Liu, Y. Zhang, S. Li, J. Huang, Y. Zeng, Z. Huang, C. Jin, N. Fu, Q. Zhao, Y. Mu, et al., Natural intestinal metabolite xylitol reduces BRD4 levels to mitigate renal fibrosis, Clinical and translational science 17 (3) (2024) e13770.
[22] M.S. Stratton, R.A. Bagchi, M.B. Felisbino, R.A. Hirsch, H.E. Smith, A.S. Riching, B.Y. Enyart, K.A. Koch, M.A. Cavasin, M. Alexanian, K. Song, J. Qi, M. E. Lemieux, et al., Dynamic chromatin targeting of BRD4 stimulates cardiac fibroblast activation, Circ. Res. 125 (7) (2019) 662–677.
[23] V. Pooladanda, S. Thatikonda, S.P. Muvvala, G. Devabattula, C. Godugu, BRD4 targeting nanotherapy prevents lipopolysaccharide induced acute respiratory distress syndrome, International journal of pharmaceutics 601 (2021) 120536.
[24] N. Kondo, Y. Nagano, A. Hasegawa, M. Ishizawa, K. Katagiri, T. Yoneda, T. Masuda, M. Kannagi, Involvement of EZH2 inhibition in lenalidomide and pomalidomide-mediated growth suppression in HTLV-1-infected cells, Biochemical and biophysical research communications 574 (2021) 104–109.
[25] J. Gu, Y. Zhang, X. Wang, J. Xiang, S. Deng, D. Wu, J. Chen, L. Yu, Y. Zhou, Y. Wang, J. Shen, Matrine inhibits the growth of natural killer/T-cell lymphoma cells by modulating CaMKIIγ-c-Myc signaling pathway, BMC complementary medicine and therapies 20 (1) (2020) 214.
[26] Y. Zhu, Y. Feng, GRAIL inhibits the growth, migration and invasion of lung adenocarcinoma cells by modulating STAT3/C-MYC signaling pathways, Journal of BUON : official journal of the Balkan Union of Oncology 26 (2) (2021) 353–358.
[27] Y. Zhu, E. Zhang, H. Gao, C. Shang, M. Yin, M. Ma, Y. Liu, X. Zhang, X. Li, Resistomycin inhibits wnt/β-catenin signaling to induce the apoptotic death of human colorectal cancer cells, Mar. Drugs 21 (12) (2023).

[28] M. Katayama, T. Fukuda, T. Kaneko, Y. Nakagawa, A. Tajima, M. Naito, H. Ohmaki, D. Endo, M. Asano, T. Nagamine, Y. Nakaya, K. Saito, Y. Watanabe, et al., Induced pluripotent stem cells of endangered avian species, Commun. Biol. 5 (1) (2022) 1049.
[29] Z. Zhu, J. Xu, L. Li, W. Ye, G. Xu, B. Chen, J. Zeng, J. Li, Z. Huang, Effect of gastric cancer stem cell on gastric cancer invasion, migration and angiogenesis, International journal of medical sciences 17 (13) (2020) 2040–2051.
[30] Y. Zhang, Y. Liu, W. Yan, X. Zhang, Y. Hou, Z. Zhou, R. Guo, G. Liu, J. Ma, Human induced pluripotent stem cell line from fibroblasts (HEBHMUi015-A) and chondrogenic differentiation, Stem Cell Res. 72 (2023) 103201.